Global climate change trends detected in indicators of ocean ecology

B. B. Cael[1,*], Kelsey Bisson[2], Emmanuel Boss[3], Stephanie Dutkiewicz[4], and Stephanie Henson[1]

1. National Oceanography Centre, Southampton, UK. 2. Department of Botany and Plant Pathology, Oregon State University, Corvallis, OR, USA. 3. University of Maine, Orono, ME, USA. 4. Massachusetts Institute of Technology, Cambridge, MA, USA.

*cael@noc.ac.uk.

Author Contributions: Cael lead and all other authors assisted with all aspects of this work.

Article Type: Report.

Short title: Climate trends in ocean color

One-Sentence Summary: Multivariate statistics reveal significant 20-year trends in ocean color over much of the ocean; a state-of-the-art ecosystem model attributes these to climate change.

Keywords: Ocean color. Climate change. Trend detection. Remote sensing.

Data Availability: Remote sensing data area available from `https://oceancolor.gsfc.nasa.gov`. Model outputs are available from `https://doi.org/10.7910/DVN/08OJUV`. Code will be made available at `https://www.github.com/bbcael` and given a Zenodo DOI should this manuscript be accepted for publication.

Conflicts: The authors have no competing interests to declare.

Acknowledgments: Cael and Henson acknowledge support from the European Union's Horizon 2020 Research and Innovation Programme under grant agreement No. 820989 (project COMFORT). The work reflects only the authors' view; the European Commission and their executive agency are not responsible for any use that may be made of the information the work contains.

Abstract

Climate change-driven trends in phytoplankton populations, as viewed by Earth-observing satellites, were thought to be masked by strong natural variability, so that >30 years of continuous data was needed to detect a climate trend. Here we show that climate change trends emerge more rapidly in ocean color (remote sensing reflectance, R_{rs}), as R_{rs} is multivariate and some wavebands have low interannual variability. We find significant trends in a twenty-year time-series of R_{rs} from the MODIS-Aqua satellite over 52% of the global surface ocean, primarily equatorward of 40°. The climate change signal in R_{rs} emerges after twenty years in similar regions covering a similar fraction of the ocean in a state-of-the-art ecosystem model, implying that the observed trends may indeed be driven by climate change. Ocean color may thus be a sentinel of climate change in surface ocean ecology and biogeochemistry.

Climate change is causing alterations in ecosystems, and is expected to increasingly cause such changes in the future [1]. Surface ocean ecosystems cover 70% of Earth's surface and are responsible for approximately half of global primary production [2]. Such communities are known to be changing at specific locations where long-term data are available [3, 4]. Detecting climate change-driven trends in ocean ecosystems on a global scale, however, is challenging because of the difficulties of making oceanographic measurements at sufficient spatial and temporal scales.

Satellite remote sensing is the only means to obtain global scale time series of marine ecosystems, as it is the only way to obtain measurements on the required spatial and temporal scales. Ocean color satellites, which measure the amount of light reflected from the earth's surface, have been collecting global measurements for several decades. A great deal of research has focused on detecting long-term trends in ocean color data, particularly in chlorophyll-a (Chl) and primary productivity over large regions [5, 6, 7, 8, 9]. However, several studies have shown that 30+ years are required to detect climate change-driven trends in satellite-derived Chl [μg/L] [10, 11, 12], even on regional scales. Chl provides information on the abundance of phytoplankton (the photosynthesizing microscopic organisms in the ocean), and is estimated from ocean color measurements as the ratio of blue versus green light emanating from the ocean [13]. Detecting climate change trends from satellite Chl, the principal product derived from ocean color, has so far not been possible. This is because no single satellite mission has lasted a sufficient duration, and there are technical issues with the intercalibration of merged multi-satellite products that complicate robust, quantitative trend detection [14, 12, 15]. Advances in statistical methods have allowed the detection of trends in large-scale regional Chl averages [16], but it is difficult to distinguish for a given location whether Chl is or is not changing, and to attribute this to climate change.

That said, the MODIS-Aqua (MOderate Resolution Imaging Spectroradiometer) satellite has far surpassed its originally planned mission duration, having just completed twenty full years of high-quality global ocean color data collection. The key variable provided by MODIS-Aqua (and any ocean color sensor) is remotely sensed reflectance (R_{rs}) which is the ratio of upwelling radiance to downwelling irradiance incident on the ocean surface. MODIS-Aqua sensors measure R_{rs} in several wavebands within the visible spectrum from 412nm in the blue part of the spectrum to 678nm in the red.

The 20 year MODIS-Aqua record constitutes a truly unique dataset and presents an opportunity to revisit the possibility of detecting and attributing climate change trends in satellite ocean color. The principal reasons one might expect this to be possible are that 1) R_{rs} is multivariate, being measured by MODIS-Aqua at several wavebands, whereas Chl is univariate, meaning R_{rs} potentially encapsulates a stronger signal than Chl (Figure S1), and 2) some R_{rs} wavebands exhibit lower interannual variability than Chl [11], meaning R_{rs} potentially has lower noise. In a complex global ocean ecosystem model, climate change driven trends in R_{rs} have been shown to indicate changes in phytoplankton community structure and become distinguishable from natural variability more rapidly than trends in Chl [11]. However, these multivariate advantages may not be sufficient to permit detection of trends because R_{rs} is known to be strongly correlated between different wavebands [17], reducing the effective dimension of the measurement, and autocorrelation in R_{rs} may persist even at the annual timescale, reducing the effective sample size of a given R_{rs} time-series. Solutions to both of these issues are possible however. Multivariate regression allows the trends (and uncertainties in those trends) in multiple variables to be estimated simultaneously, while accounting for correlations between dependent variables [18]. Methods also exist to account for autocorrelation in regression analysis, such as the Cochrane-Orcutt procedure [19], which estimates and subtracts the autoregressive component. In essence, then, such a regression maximizes the signal (number of simultaneous variables) used to detect a trend while also minimizing the noise (interannual variability in those variables) and accounting for correlations between variables and years.

To investigate possible trends in ocean color, we performed such an autocorrelation-corrected multivariate regression on the first twenty years of MODIS-Aqua ocean R_{rs} spanning July 2002 – June 2022 (Materials and Methods). We find significant trends, here defined as a signal-to-noise ratio (SNR) greater than two, in 51.9% of the ocean, primarily equatorward of 40° (Figure 1). In contrast, only a small fraction of this portion of the ocean has significant trends in Chl (9.5%, green stippling in Figure 1), such that even if the green stippled areas in Figure 1 are excluded, more than a quarter of the total ocean area has a significant trend in ocean color.

We also note that these trends are not strongly associated with changes in sea surface temperature (SST, °C). When the same analysis is performed for MODIS-Aqua-based SST (Materials and Methods), we find significant trends in SST in 23.1% of the ocean. However, only 22.6% of the ocean area with a significant trend in R_{rs} has a significant trend in SST, and only 49.5% of the ocean area with a significant trend in SST has a significant trend in R_{rs}, whereas 23.1% and 51.9% respectively would be expected to if trends in R_{rs} were unrelated to trends in SST. This suggests that the detected changes in R_{rs} are not driven by changes in SST. Instead, R_{rs} changes may be due to other drivers such as changing mixed layer depth or upper ocean stratification [20]. These are known to affect plankton communities and expected to change with climate, but harder to detect trends in over shorter time periods (i.e. 20 years) because they are measured less precisely than SST.

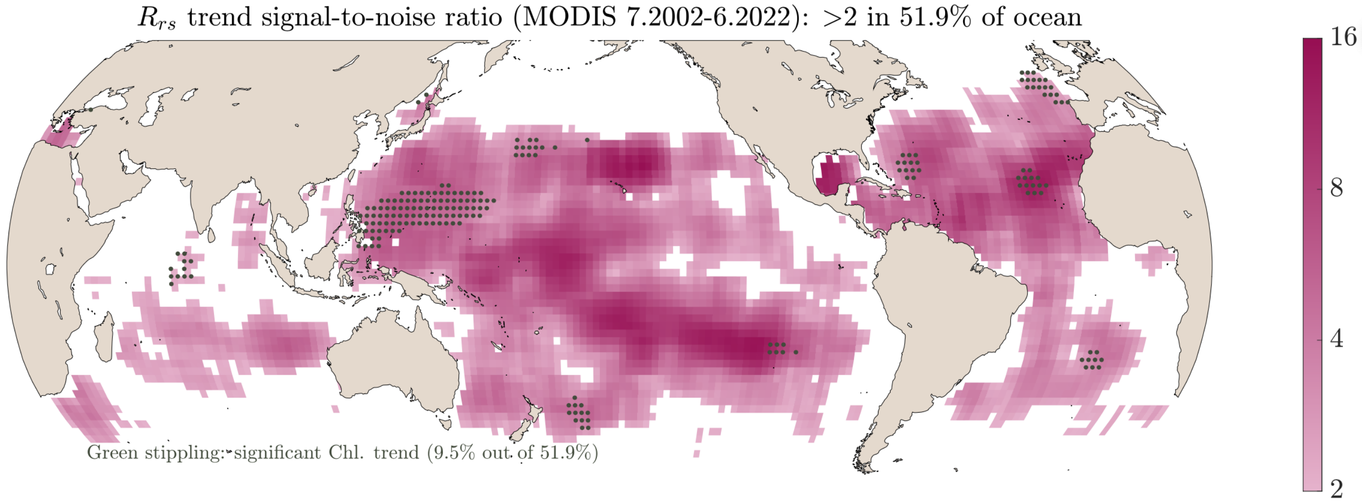

Figure 1: Map of locations where ocean color trend signal-to-noise ratio (SNR) is >2 for 20-year annual time series. Intensity of purple color indicates the SNR. Green stippling indicates regions with significant chlorophyll trends.

We find that a vast swathe of the ocean has a significant trend in R_{rs}, when considering many wavebands at the same time. Significant trends tend to occur in low-'noise,' (i.e. weak interannual variability) subtropical and tropical regions, rather than high-'signal' regions (Figure S2). The likelihood of SNR *exceeding* 2 and a trend being detectable increases with decreasing noise levels, but does not increase with increasing signal levels. Significant trends are also spectrally broad-based across wavebands and not linked to any particular waveband (Figures S3 and S4). Given the difficulties and associated uncertainties in converting R_{rs} to Chl and other products such as ocean optical properties or phytoplankton carbon, it is a challenge to interpret these trends ecologically and/or biogeochemically [21, 22]. However, ocean color does encode combined information about surface ecosystems, dissolved and particulate organic matter, and the identified trends suggest that these have significantly changed over the past twenty years.

The primary question of interest is whether the identified trends are driven by climate change specifically. To test this, we performed the same analysis on MODIS-like R_{rs} simulated by a numerical model of a complex global ocean ecosystem and associated biogeochemical cycles [23, 11]. The model simulates the changes to the marine ecosystem and optics over the course of the 21st Century under a high greenhouse emission scenario (see methods). By also considering a control simulation (i.e. without perturbation from increased emissions) we can attribute any changes to be driven by climate change. We analyzed this model in terms of the time of emergence (ToE [years]) [24], which quantifies how long it takes for the climate-change-driven trend in a simulation with climate change (i.e. a forced simulation) to emerge (with a signal-to-noise ratio of 2) from the natural variability in a simulation without climate change (i.e. a control simulation), both over the period 2000-2105. For the model R_{rs}, the ToE≤20 years in 45.6% of the ocean, a comparable fraction to the 51.9% of the ocean for which we find a significant trend in MODIS-Aqua R_{rs} (Figure 2). The (area-weighted) median ToE across the entire model surface ocean is 22.3 years. Furthermore, while the coarse resolution of the model would call into question any precise spatial comparison with observations, similar broad regions in both cases are responsible for the significant trends after twenty years, notably the North Atlantic

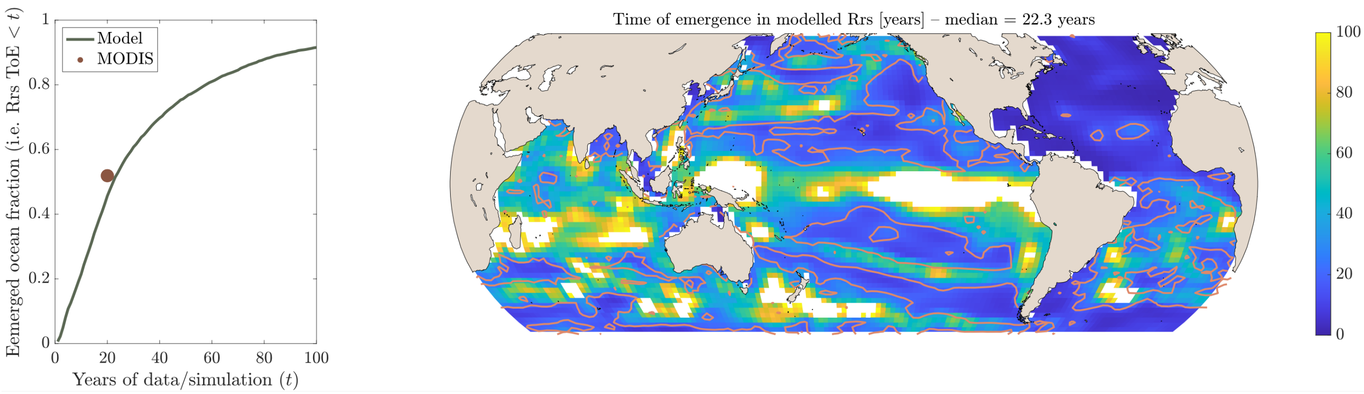

Figure 2: Left: cumulative distribution function of the time of emergence (ToE) of the ocean color trend in the model simulation. Orange point indicates fraction of total surface ocean area with a significant trend in the 20-year MODIS-Aqua time-series. Right: map of ToE in the model simulation. Orange lines are the 20-year ToE contour. See [11] for a similar plot for Chl.

and the subtropical Pacific. While this is arguably the only numerical model suitable for such investigations, limiting the strength of any attribution statement that can be made from it, the consistency in overall extent and general location of significant trends in the observations and emerged climate change-driven trends in the model suggest that the observed trends are indeed climate change-driven. Furthermore, as these changes in R_{rs} have previously been shown to be associated with community structure changes in the model [11], which emerge faster than Chl trends or those of other optically relevant properties, this consistency suggests the observed R_{rs} changes may be indicative of changes in phytoplankton community structure. Climate driven changes to phytoplankton community structure would likely have knock-on effects on food webs, biogeochemical cycles and marine biodiversity.

These results imply that climate change effects are already being felt in surface phytoplankton populations, but have not yet been detected since previous studies have considered Chl or other univariate approaches. This may indicate that ocean color (R_{rs}) is a ‘sentinel’ for ocean climate change, particularly for surface ocean ecology and biogeochemistry, as has been argued for lakes [25]. This is because, similar to lakes, R_{rs} integrates and is sensitive to climate-driven changes in properties of interest, facilitating early detection of climate change signals. R_{rs}, and thus surface ocean ecology, has changed significantly over a large fraction of the ocean over the past twenty years, possibly due to climate change and in the form of changing phytoplankton community structure. Such changes have potential implications both for the role of plankton in marine biogeochemical cycles and thus ocean carbon storage, and for plankton consumption by higher trophic levels and thus fisheries. These changes are consistent with expected changes in drivers such as mixed layer depth and upper ocean ocean temperature and stratification, but may be more easily detectable on the global scale as we have done here thanks to the multivariate nature of R_{rs}. This highlights the value of long-term satellite missions like MODIS-Aqua and of space agencies maintaining missions for as long as feasible. That significant trends occur primarily where interannual variability is low means that a similar signal may be expected to emerge in other portions of the ocean in coming years, though unfortunately the MODIS-Aqua mission is scheduled to end in the near future. For instance, our model results (Figure 2, left panel) suggest that another 6 years of MODIS-Aqua data, the originally scheduled mission length, would reveal significant changes in another 10% of the ocean. While the remote sensing reflectance trends detected here are challenging to interpret given the difficulties and additional uncertainties involved in translating remote sensing reflectances into derived products, ongoing work (e.g. [26]) linking remote sensing reflectance to phytoplankton community composition in particular may shed light on what the trends found here indicate about changing surface ocean ecosystem structure [27, 28]. Given the key role of planktonic ecosystems to marine food webs, global biogeochemical cycles, and carbon cycle-climate feedbacks, a sentinel of change in these ecosystems is of great utility.

Materials and Methods

We generated a twenty year annual time-series of MODIS-Aqua R_{rs} and Chl by extracting the monthly level-3, 4km R_{rs} and Chl values from July 2002 to June 2022 from `https://oceancolor.gsfc.nasa.gov/`. We use the seven ocean wavebands for MODIS-Aqua centered at 412nm, 443nm, 488nm, 531nm, 547nm, 667nm, and 678nm (`https://modis.gsfc.nasa.gov/about/specifications.php`). The 2022 reprocessing of R_{rs} and Chl was used, which reduces atmospheric correction errors and, crucially, minimizes any instrumental drift through updated sensor calibrations. Monthly data were aggregated into years each beginning in July, and data were averaged spatially to 2° resolution, resulting in a 90-by-180-by-20-by-10 array (respectively latitude, longitude, year, and waveband), and a 90-by-180-by-20 array for Chl. MODIS-Aqua was selected because it is now a twenty-year record, the longest single-satellite R_{rs} product available; merged products were not considered because of the known issues with satellite intercalibration, which are challenging to deal with quantitatively in detecting significant trends over time [12]. MODIS-Aqua also provides a daytime sea surface temperature (SST, °C) product, for which we generated a comparable time-series (i.e. 20 July-June years at 2° spatial resolution).

For each 2°-by-2° grid cell, we then performed a multivariate regression of R_{rs} versus time. Before performing the regression, the serial autocorrelation in the signal was removed using the Cochrane-Orcutt procedure [19]. For locations with significant autocorrelation (42% of grid cells), one iteration was applied, and then a second iteration was applied for grid cells whose autocorrelation continued to be significant (9% of grid cells). No more than two iterations was applied to any grid cell because <2% of grid cells had significant autocorrelation at the 5% level after the application of zero-to-two iterations to all grid cells. Our conclusions are not affected by this choice; for instance, applying one iteration to all grid cells equally yielded a negligible difference. The same approach is applied to the Chl time series. We then calculate the SNR in each case according to

$$SNR = \frac{\sqrt{\sum_i b_i^2}}{\sqrt{\frac{\vec{b}}{\sqrt{\sum_i b_i^2}} C \left(\frac{\vec{b}}{\sqrt{\sum_i b_i^2}} \right)'}}$$

where $\vec{b}$ is the vector of trend estimates for each waveband and C is the variance-covariance matrix of $\vec{b}$. In other words the signal to noise ratio SNR is the magnitude of the multivariate trend vector (see Figure S1), divided by the projection along this vector of the multivariate uncertainty of this multivariate trend. For Chl, i.e. the univariate case, this reduces to $SNR = b/C$, where b is the magnitude of the trend and C is the uncertainty of this trend.

For Figure S3 we performed the same procedure as above for each individual MODIS-Aqua waveband of R_{rs}. Figure S4 is identical to Figure S3 but with locations where $SNR < 2$ for all wavebands removed, to show that individual wavebands have significant trends in small and overlapping regions, underscoring that the detected trends are due to the multivariate nature of R_{rs} and not associated with any individual waveband. We also performed this analysis for SST to compute the overlap between significant trends in R_{rs} and SST as described in the main text.

The biogeochemical model is the same as used in [11]. This is a complex ocean ecosystem and biogeochemistry model, resolving the major elemental cycles and eight phytoplankton types. The ecosystem/biogeochemistry is forced with output from an earth system model of intermediate complexity [29]. From an 1860 spinup, two simulations are performed: one is a control simulation run with constant 1860 greenhouse gas concentrations, and a second is run with high-emissions scenario with increasing greenhouse gas concentrations (Representative Concentration Pathway 8.5-like). Thus the differences between the simulation indicate anthropogenically-driven climate change. Each simulation is run for 250 years, nominally 1860 to 2110, and the analysis described here was performed on the last 106 years (i.e. nominally from 2000 to 2105). The model resolves radiative transfer as described in [23] to generate R_{rs} at 25nm resolution from 400–700nm, which we linearly interpolate to the MODIS-Aqua spectral waveband peaks (412, 443, 469, 488, 531, 547, 555, 645, 667, 678nm). Linearly interpolating the spectra to 1nm resolution and convolving with the MODIS-Aqua spectral response functions did not affect the result. The model's spatial resolution is 2°-by-2.5° with 22 vertical layers. The ocean physics displays a realistic year-to-year variability in surface temperature and produces interannual variability (e.g. El Nino-Southern Oscillation) with frequency, seasonality, magnitude and patterns in general agreement with observations. Because of the high computational demand of this model, we use a single climate simulation from an ensemble of perturbed physics, perturbed initial conditions, and varied emissions scenarios, with medium effective climate sensitivity of approximately 3.0°C [29]. The control simulation showed that there were no significant drifts in the ecological or optical properties discussed here. We refer to [11] and references therein for further details and model validation.

Using this model we perform the same multivariate regression as above. We then calculate, following [11] and others, the time of emergence (ToE) for each grid cell according to ToE = 2×(standard deviation)/(trend), where the standard deviation is that of the annual means at any grid location in the control run and the trend is that of the full forced simulation. Calculating and removing any drift in the control simulation negligibly affected this calculation.

References

[1] Sarah Cooley et al. "Oceans and coastal ecosystems and their services". In: *IPCC AR6 WGII*. Cambridge University Press, 2022.

[2] Christopher B Field et al. "Primary production of the biosphere: integrating terrestrial and oceanic components". In: *science* 281.5374 (1998), pp. 237–240.

[3] Lukas Jonkers, Helmut Hillebrand, and Michal Kucera. "Global change drives modern plankton communities away from the pre-industrial state". In: *Nature* 570.7761 (2019), pp. 372–375.

[4] Julia A Jones and Charles T Driscoll. "Long-term ecological research on ecosystem responses to climate change". In: *BioScience* 72.9 (2022), pp. 814–826.

[5] Andrew J Irwin and Matthew J Oliver. "Are ocean deserts getting larger?" In: *Geophysical Research Letters* 36.18 (2009).

[6] Elodie Martinez et al. "Climate-driven basin-scale decadal oscillations of oceanic phytoplankton". In: *Science* 326.5957 (2009), pp. 1253–1256.

[7] Michael J Behrenfeld et al. "Climate-driven trends in contemporary ocean productivity". In: *Nature* 444.7120 (2006), pp. 752–755.

[8] Watson W Gregg and Cécile S Rousseaux. "Decadal trends in global pelagic ocean chlorophyll: A new assessment integrating multiple satellites, in situ data, and models". In: *Journal of Geophysical Research: Oceans* 119.9 (2014), pp. 5921–5933.

[9] Charles R McClain. "A decade of satellite ocean color observations". In: *Annu. Rev. Mar. Sci* 1.1 (2009), pp. 19–42.

[10] Stephanie A Henson et al. "Detection of anthropogenic climate change in satellite records of ocean chlorophyll and productivity". In: *Biogeosciences* 7.2 (2010), pp. 621–640.

[11] Stephanie Dutkiewicz et al. "Ocean colour signature of climate change". In: *Nature communications* 10.1 (2019), pp. 1–13.

[12] Claudie Beaulieu et al. "Factors challenging our ability to detect long-term trends in ocean chlorophyll". In: *Biogeosciences* 10.4 (2013), pp. 2711–2724.

[13] John E O'Reilly. *SeaWiFS postlaunch calibration and validation analyses, part 3*. NASA Center for AeroSpace Information, 2000.

[14] David Antoine et al. "Bridging ocean color observations of the 1980s and 2000s in search of long-term trends". In: *Journal of Geophysical Research: Oceans* 110.C6 (2005).

[15] Bertrand Saulquin et al. "Detection of linear trends in multisensor time series in the presence of autocorrelated noise: Application to the chlorophyll-a SeaWiFS and MERIS data sets and extrapolation to the incoming Sentinel 3-OLCI mission". In: *Journal of Geophysical Research: Oceans* 118.8 (2013), pp. 3752–3763.

[16] Matthew L Hammond et al. "Regional surface chlorophyll trends and uncertainties in the global ocean". In: *Scientific reports* 10.1 (2020), pp. 1–9.

[17] Yannick Huot and David Antoine. "Remote sensing reflectance anomalies in the ocean". In: *Remote Sensing of Environment* 184 (2016), pp. 101–111. ISSN: 0034-4257. DOI: `https://doi.org/10.1016/j.rse.2016.06.002`. URL: `https://www.sciencedirect.com/science/article/pii/S0034425716302310`.

[18] James Douglas Hamilton. *Time series analysis*. Princeton university press, 2020.

[19] Donald Cochrane and Guy H Orcutt. "Application of least squares regression to relationships containing auto-correlated error terms". In: *Journal of the American statistical association* 44.245 (1949), pp. 32–61.

[20] Paul G Falkowski and Matthew J Oliver. "Mix and match: how climate selects phytoplankton". In: *Nature reviews microbiology* 5.10 (2007), pp. 813–819.

[21] P Jeremy Werdell et al. "An overview of approaches and challenges for retrieving marine inherent optical properties from ocean color remote sensing". In: *Progress in oceanography* 160 (2018), pp. 186–212.

[22] Timothy S Moore, Janet W Campbell, and Mark D Dowell. "A class-based approach to characterizing and mapping the uncertainty of the MODIS ocean chlorophyll product". In: *Remote Sensing of Environment* 113.11 (2009), pp. 2424–2430.

[23] S Dutkiewicz et al. "Capturing optically important constituents and properties in a marine biogeochemical and ecosystem model". In: *Biogeosciences* 12.14 (2015), pp. 4447–4481.

[24] Irina Mahlstein et al. "Early onset of significant local warming in low latitude countries". In: *Environmental Research Letters* 6.3 (2011), p. 034009.

[25] Rita Adrian et al. "Lakes as sentinels of climate change". In: *Limnology and oceanography* 54.6part2 (2009), pp. 2283–2297.

[26] Sasha J Kramer and David A Siegel. “How can phytoplankton pigments be best used to characterize surface ocean phytoplankton groups for ocean color remote sensing algorithms?” In: *Journal of Geophysical Research: Oceans* 124.11 (2019), pp. 7557–7574.

[27] P Jeremy Werdell, Collin S Roesler, and Joaquim I Goes. “Discrimination of phytoplankton functional groups using an ocean reflectance inversion model”. In: *Applied optics* 53.22 (2014), pp. 4833–4849.

[28] Shubha Sathyendranath et al. “Phytoplankton functional types from Space.” In: (2014).

[29] Erwan Monier et al. “An integrated assessment modeling framework for uncertainty studies in global and regional climate change: the MIT IGSM-CAM (version 1.0)”. In: *Geoscientific Model Development* 6.6 (2013), pp. 2063–2085.

Supplementary Figures

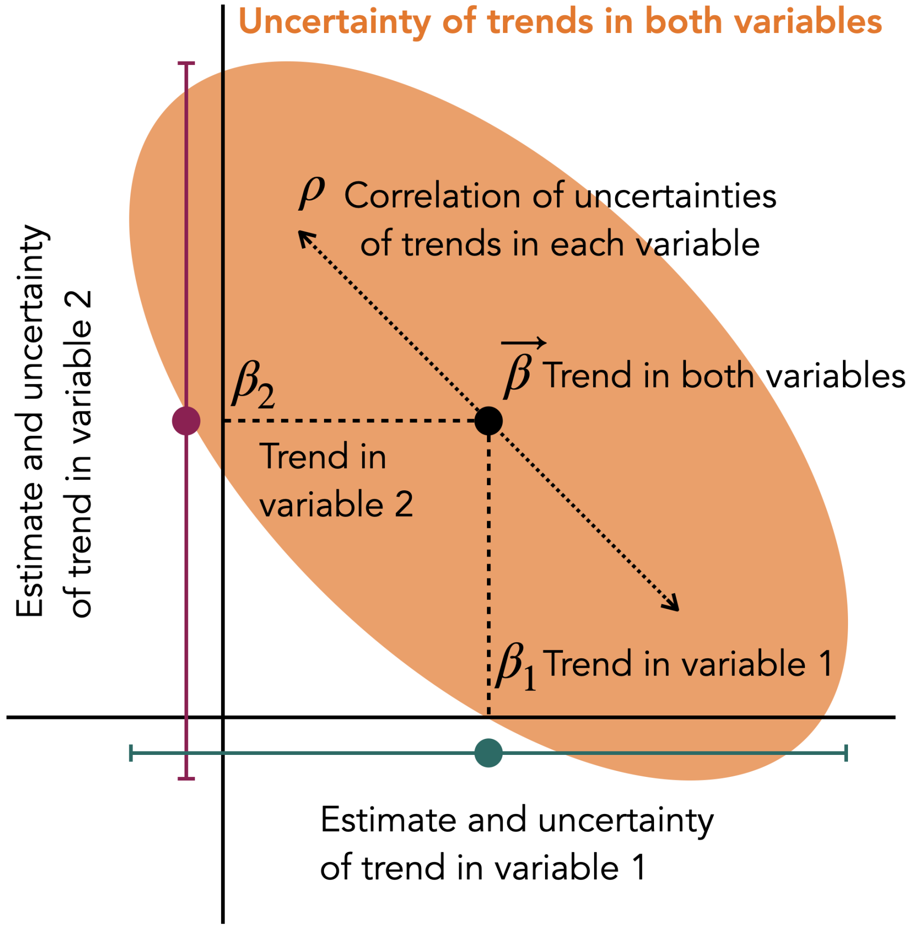

Supplementary Figure 1: Schematic of multivariate trend detection in two-dimensional case. Teal and purple points and error bars indicate estimates and uncertainties of trends in two different variables, β_1 and β_2. Black point and orange ellipse indicate estimate and uncertainty in the two-dimensional variable $\vec{\beta} = (\beta_1, \beta_2)$. Dotted arrow indicates correlation (ρ) between uncertainties of estimates in each variable. In this graphical illustration, estimated trends in β_1 and β_2 are not significant, but the estimated trend in $\vec{\beta}$ is.

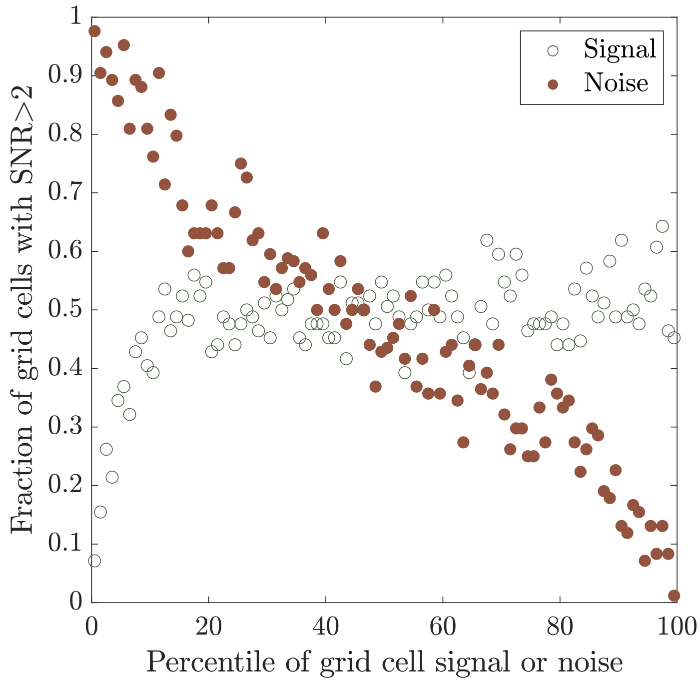

Supplementary Figure 2: Scatterplot of the fraction of grid cells with signal-to-noise ratios >2 versus the percentile of grid cells' 'signal' (i.e. the magnitude of the trend, empty green points) and 'noise' (i.e. the uncertainty in the trend, filled orange points). Lower-'noise' regions more often have signal-to-noise ratios >2, whereas high-'signal' regions more often have signal-to-noise ratios <2, indicating that places with significant trends are those with the lowest trend uncertainty, due to low interannual variability, rather than because they have the strongest trends.

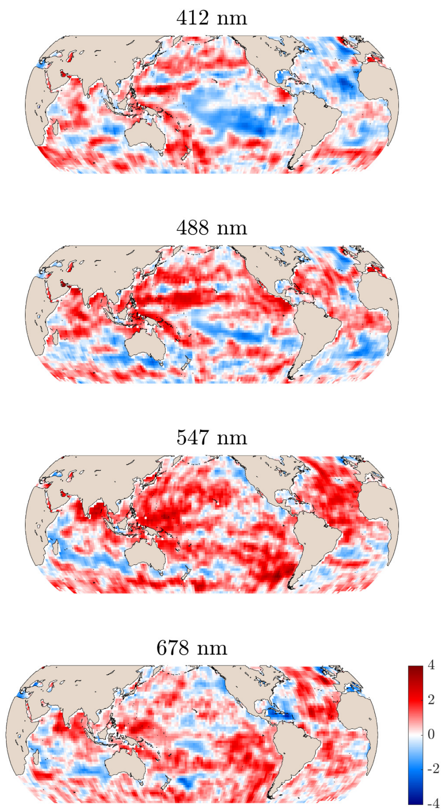

Supplementary Figure 3: Maps of the signal-to-noise ratio of univariate regressions of each wavelength, with Cochrane-Orcutt procedure applied. Blue/red indicates a negative/positive trend, and intensity of color indicates the signal-to-noise ratio.

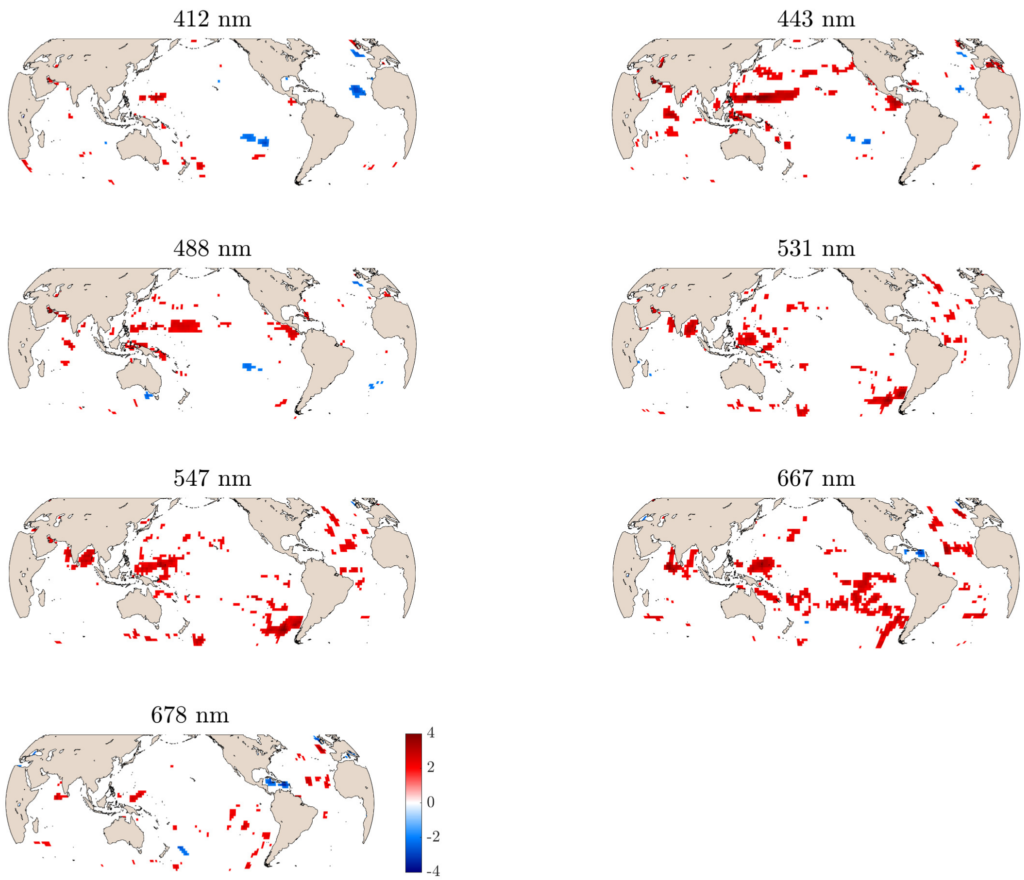

Supplementary Figure 4: Same as Figure S3 but where only locations with $SNR > 2$ are colored in.